Optical Materials: X 20 (2023) 100274

Contents lists available at ScienceDirect

Optical Materials: X

journal homepage: www.journals.elsevier.com/optical-materials-x

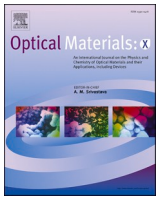

Femtosecond laser induced damage threshold and incubation in L-threonine aminoacid crystal

L.K. Nolasco [a,b,1], G.A. Flores [b,1], S.N.C. Santos [b], M.B. Andrade [b,c], J.J. Rodrigues Jr. [d], C. R. Mendonça [b,*]

[a] Department of Materials Engineering, School of Engineering of São Carlos, University of São Paulo, PO Box 359, 13563-120, São Carlos, SP, Brazil
[b] São Carlos Institute of Physics, University of São Paulo, PO Box 369, 13561-970, São Carlos, SP, Brazil
[c] Physics Department, Federal University of Ouro Preto, Ouro Preto, MG, 35400-000, Brazil
[d] Federal University of Sergipe, Physics Department, 49107-230, São Cristóvão, SE, Brazil

ARTICLE INFO

Keywords:
Fs-micromachining
Nonlinear optics
Organic crystal
Incubation effect
L-threonine

ABSTRACT

L-threonine aminoacid crystals exhibit high second-order optical nonlinearities that can be exploited for second harmonic generation, optical parametric amplification, and optical parametric oscillation. In addition, it possesses a large transparency window and low refractive index, making them an attractive material for photonics devices. Among several processing methods used to develop photonic integrated micro-devices, fs-laser micromachining has stood out for its high resolution, either on the surface or in the bulk, as well as to its flexibility to be used with various types of materials. Although organic crystals present relevant linear and nonlinear optical features, studies on fs-laser processing in such materials are yet scarce. Thus, this work presents a study of the fs-laser incubation and damage threshold fluence determination in L-threonine crystals at 515 nm and 1030 nm. The damage threshold fluence was determined for one up to 10^5 pulses. For the single pulse regime, we obtained $F_{th} = (0.94 \pm 0.04)$ J/cm^2 at 1030 nm and $F_{th} = (0.31 \pm 0.01)$ J/cm^2 at 515 nm. Such difference is explained by the number of photons involved in each case; 5-photons at 1030 nm and 3-photons at 515 nm. Also, a slower incubation dynamic was observed at 515 nm. Still, micro-Raman spectroscopy revealed that no structural modifications were induced by the fs-laser pulses on the sample upon micromachining. Such results provide relevant data for the processing of L-threonine crystals via fs-laser micromachining to achieve organic photonic integrated devices.

1. Introduction

Organic materials play a fundamental role in the development of novel technologies in photonics for offering exciting features, such as ease of functionalization, high optical nonlinearities, and fast response times [1–6]. Amino acid organic crystals, specifically, exhibit high second-order nonlinear optical properties [7–9], which can be exploited for second harmonic generation (SHG), optical parametric amplification (OPA), and optical parametric oscillation (OPO) [10]. The third-order optical nonlinearities in amino acids have been determined by the *Z*-scan technique with femtosecond laser pulses [11], revealing a nonlinear refractive index ranging from 10^{-17} up to 10^{-16} cm^2/W. Besides, organic crystals exhibit a smaller refractive index than their inorganic counterparts, resulting in reduced insertion losses, an interesting feature for integrated devices. For such reasons, amino acid crystals have been drawing considerable attention as potential materials in photonics.

Numerous techniques have been developed to accomplish miniaturized photonic integrated devices, ranging from conventional lithography to direct laser writing [12,13]. Among these approaches, fs-laser processing has been prompted as a relevant tool to fabricate optical devices because of its high precision in producing sub-micron/micron structures on the surface or in the bulk of a material [14]. Consequently, fs-laser direct writing has been used to fabricate waveguides, resonators, lasers, filters, sensors, in a myriad of materials, from polymers to semiconductors [1,14–18]. Although amino acid organic crystals are interesting linear and nonlinear optical materials, studies on fs-laser processing in such materials remains scarce. To the best of our

* Corresponding author.
E-mail address: crmendon@ifsc.usp.br (C.R. Mendonça).
[1] These authors contributed equally to this work.

https://doi.org/10.1016/j.omx.2023.100274
Received 30 July 2023; Received in revised form 30 September 2023; Accepted 3 October 2023
Available online 13 October 2023

knowledge, the sole existing work in this direction is the inscription of cladding waveguides in L-threonine crystals using femtosecond pulses at 800 nm [19].

In this work, we present a study of the fs-laser incubation and damage threshold fluence (F_{th}) of L-threonine crystals at 515 nm and 1030 nm, whose difference is associated with the number of photons involved in the multi-photon ionization. Micro-Raman spectroscopy revealed that no structural changes were induced by the fs-laser pulses on the sample upon micromachining. Therefore, this paper provides the necessary data for the processing of L-threonine crystals with fs-laser pulses, that can be used for the fabrication of photonic devices, since laser operation near the damage threshold fluence increases micromachining resolution.

2. Experimental

The L-threonine crystal was grown through the supersaturated aqueous solution technique [8]. The sample is transparent from 255 up to 1100 nm, as seen in the absorbance spectrum in Fig. 1(a), and presents a bandgap of 4.9 eV, which is in good agreement with values found in the literature [8,20,21], determined by extrapolating the region where the sample starts to absorb light seen by the red-dashed line in Fig. 1(a) or through the Tauc/Davis-Mott plot seen in Fig. 1(b), where the bandgap is determined by the intersection of the linear portion of the absorption region with the horizontal axis. Such plot relates the absorption coefficient (α) to the bandgap (E_g) as $(\alpha h\nu)^{1/b} = C(h\nu - E_g)$, where h is Planck's constant, ν is the excitation light frequency C is a constant and b indicates the nature of the electron transition which, in this case, since L-threonine's bandgap is indirect, $b = 2$ [22–24].

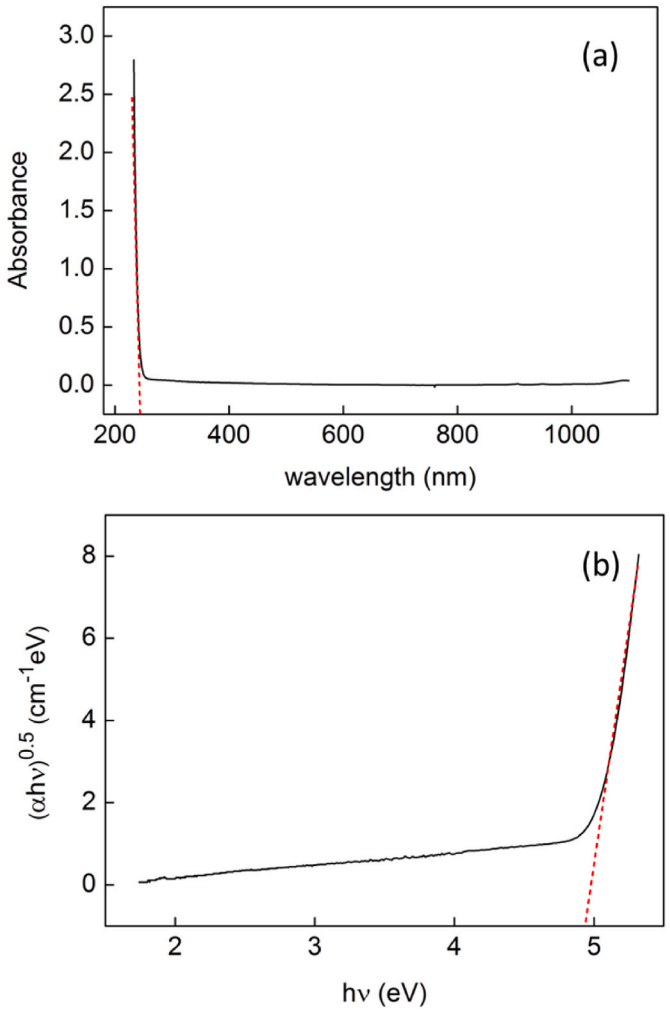

Fig. 1. Absorbance (a) and Tauc plot (b) of the L-threonine sample.

The femtosecond laser micromachining was performed by a diode-pumped Yb:KGW laser system, which emits a Gaussian beam centered at 1030 nm (fundamental) or 515 nm (second harmonic), with 216 fs of pulse duration, and repetition rate from 100 Hz up to 1 MHz (controlled by a Pockels cell-based pulse selector), at a linear polarization. The experimental setup consists of an objective lens (NA = 0.25) which focalizes the beam onto the sample, that in turn is located on a computer-controlled motorized platform. The fs-micromachining is observed in real-time through a CCD camera, and the microstructured lines were measured by optical microscopy.

Damage threshold fluence (F_{th}) was determined through the zero damage method [25]. According to such methodology, the squared half-width (r^2) of a line produced by a Gaussian beam is given by

$$r^2 = \frac{\omega_0^2}{2} \ln\left(\frac{E_p}{E_{th}}\right), \tag{1}$$

where w_0 is the Gaussian beam waist, E_p is the pulse energy, and E_{th} is the damage threshold energy. The damage threshold fluence is, then, determined by

$$F_{th} = \frac{2E_{th}}{\pi\omega_0^2}. \tag{2}$$

Thus, one can determine F_{th} by plotting r^2 as a function of E_p , whose data can be found by analyzing the width of the micromachined lines on the surface of the sample with distinct pulse energies.

The number of pulses per spot can be determined by

$$N = \vartheta_3\left(0, e^{-2\left(\frac{V}{f w_0}\right)^2}\right), \tag{3}$$

where ϑ_3 is the Jacobi theta function [26], V is the scanning speed and f is the laser's repetition rate [27–30].

Raman spectroscopy was carried out on the sample by a micro-Raman system (LabRAM HR Evolution), with a 532 nm excitation by a solid-state laser, 1800 gr/mm grating and a 100 × microscope objective lens (NA = 0.90) used to focalize the beam on the sample, which is placed on a motorized *xyz* computer-controlled translation stage.

3. Results and discussion

Fig. 2 displays the zero damage method results for L-threonine at 1030 nm (a) and 515 nm (b) for approximately 10^4 pulses. Fig. 2(right) shows the micromachined lines increasing in width (and roughness) with the increase of the applied pulse energy (from 200 up to 450 nJ at 1030 nm and from 145 up to 210 nJ at 515 nm), as seen in Refs. [27–29], and in accordance with Eq. (1). Such micromachined structures, produced at a scanning speed of 0.1 mm/s and a pulse repetition rate of 197.5 KHz, were measured through optical microscopy and the graph of the squared half-width of the lines as a function of the fs-laser pulse energy can be seen in Fig. 2(left), which resulted in the damage threshold fluence value of (0.33 ± 0.08) J/cm^2 and w_0 of (4.4 ± 0.3) μm for the 1030 nm case, and (0.10 ± 0.02) J/cm^2 and w_0 of (5.7 ± 0.2) μm for the 515 nm case, by fitting the experimental data with Eq. (1).

Thus, by repeating the previous methodology for different number of pulses per spot used to fabricate the microstructures (N) (from 1 up to 10^5) and for both wavelengths, one is able to analyze the incubation effect. The incubation effect of L-threonine at 515 nm and 1030 nm can be seen in Fig. 3(a) and (b), respectively. As expected from such cumulative effect, the damage threshold fluence decreases with the increase in the number of fs-laser pulses per area exciting the sample: at 515 nm, the damage threshold fluence decreases from (0.31 ± 0.01) J/cm^2 down to (0.05 ± 0.01) J/cm^2 with ~ 2 × 10^4 pulses, while at 1030

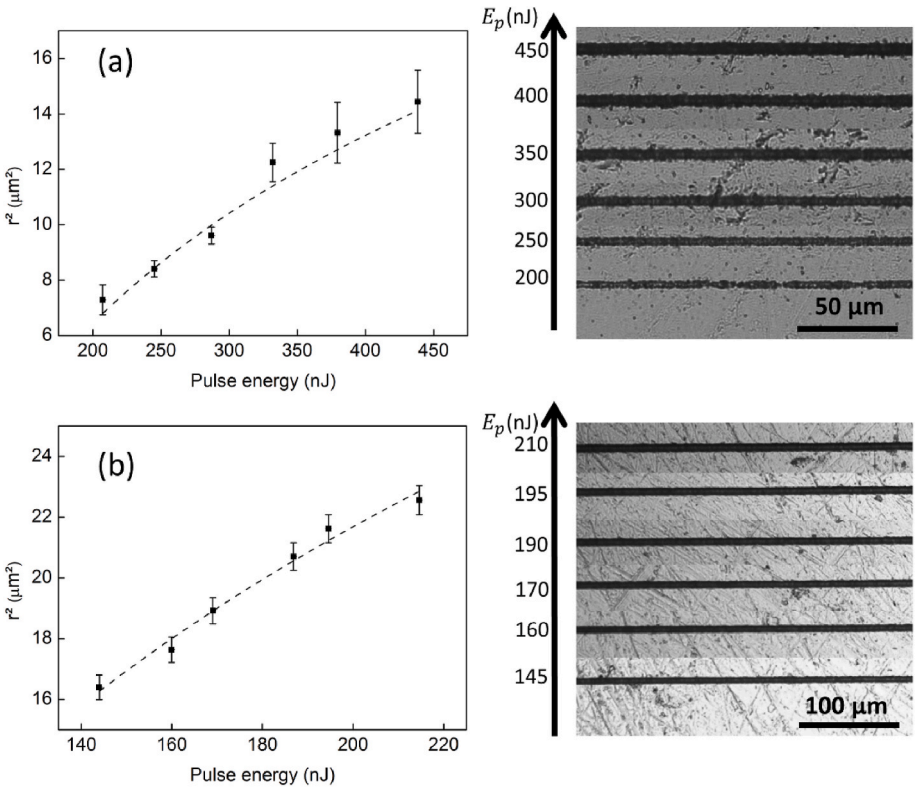

Fig. 2. Zero damage method graph of the squared half-width of the micromachined structures as a function of the applied pulse energy at 1030 nm (a) and 515 nm (b), and the measured lines for each respective graph seen in the left.

nm, it decreases from (0.94 ± 0.04) J/cm^2 down to (0.37 ± 0.04) J/cm^2 with ~ 70 pulses. The incubation effect in dieletric materials can be described by a model that considers a saturation of defects accumulation [31], given by

$$F_{th,N} = \left(F_{th,1} - F_{th,\infty}\right)e^{-k(N-1)} + F_{th,\infty}, \tag{4}$$

where the damage threshold fluence for N pulses ($F_{th,N}$) is in function of the damage threshold fluence for a single pulse ($F_{th,1}$), infinite pulses ($F_{th,\infty}$) and k, which is the incubation parameter. Such parameter indicates the efficiency to which $F_{th,1}$ reaches the $F_{th,\infty}$ value: a higher k value means that fewer fs-laser pulses are necessary to achieve the bottom plateau fluence value. Thus, the exponential defect model given by Eq. (4) was used for the fitting the incubation data seen in Fig. 3 (gray-dashed line). As such, the incubation parameter k was determined to be (2.2 ± 0.6) × 10^{-4} at 515 nm and (6 ± 2) × 10^{-2} at 1030 nm, indicating a slower incubation dynamic for excitation at 515 nm, as observed from the experimental data.

The greater damage threshold fluence value at 1030 nm for a single pulse compared to the 515 nm case is attributed to the nature of the nonlinear ionization process that leads to the fs-laser micromachining. Such process can be determined through the Keldysh parameter (γ_K), given by

$$\gamma_K = \frac{\nu}{e}\sqrt{\frac{m_e \varepsilon_0 c n_0 E_g}{I_0}}, \tag{5}$$

where ν and I_0 are the laser's frequency and peak intensity, e and m_e are the electron's charge and mass, c is the light speed, and finally n_0 is the material's refractive index [32]. From such parameter, if $\gamma_K > 1.5$, multiphoton ionization is the predominant process; otherwise, tunneling ionization prevails [33]. Thus, in this work, we determined the multiphoton ionization to be the dominant nonlinear absorption process for the single pulse case. As such, given the bandgap of 4.9 eV for the L-threonine sample, for an excitation at 515 nm, three-photon ionization is necessary for the processing of the sample, while at 1030 nm, five-photon ionization is required. As seen from Ref. [28], a multiphoton ionization process that requires a five-photon interaction is much less probable to occur than a three-photon one, thus a bigger fluence that leads to the micromachining of the sample is necessary.

A micro-Raman analysis was also performed on the sample, seen in Fig. 4, to evaluate molecular structural modifications resulting from fs-laser micromachining. Measurements were taken on the micromachined lines produced at 515 nm (green line) and 1030 nm (red line) as well as the non-irradiated region (black line). The peak found in the 530-600 cm^{-1} region is related to CO_2^- rocking; an intense peak can be found at 870 cm^{-1}, attributed to C–C–N vibration; the peaks found in the 1010-1150 cm^{-1} interval are related to CH_3 and NH_3 rocking vibration; the peaks in the 1300-1500 cm^{-1} region are related to stretching of C–O and bending of O–H, symmetric stretching of CO_2, bending vibration of CH_3, and symmetric bending of NH_3; finally, in the 2800-3100 cm^{-1} interval, the peaks are attributed to symmetric stretching of CH_3, C–H stretching, asymmetric stretching of CH_3, N–H stretching, and NH_3 streching vibrations and asymmetric stretching [34–36].

In the comparison of Raman spectra, no significant band shifts were observed, indicating that fs-laser micromachining did not significantly change the material's molecular structure. However, variations in the relative intensity ratios of certain bands can be noted. To elucidate this behavior, it's worth noting how L-threonine molecules are arranged within the crystalline structure. Similar to other amino acid crystals [37–41], hydrogen bonds between the amino groups and carboxyl oxygen atoms play a significant role in intermolecular cohesion. Therefore, the influences of hydrogen bonds on molecular cohesion can be tracked through Raman spectroscopy by examining bands associated with these interactions [42]. According to Ref. [38], hydrogen bonds may break as temperature increases, leading to differences in intensity within related bands in a L-alanine crystal. Thus, such phenomenon can explain what was observed in Fig. 4, since temperature rises abruptly during the

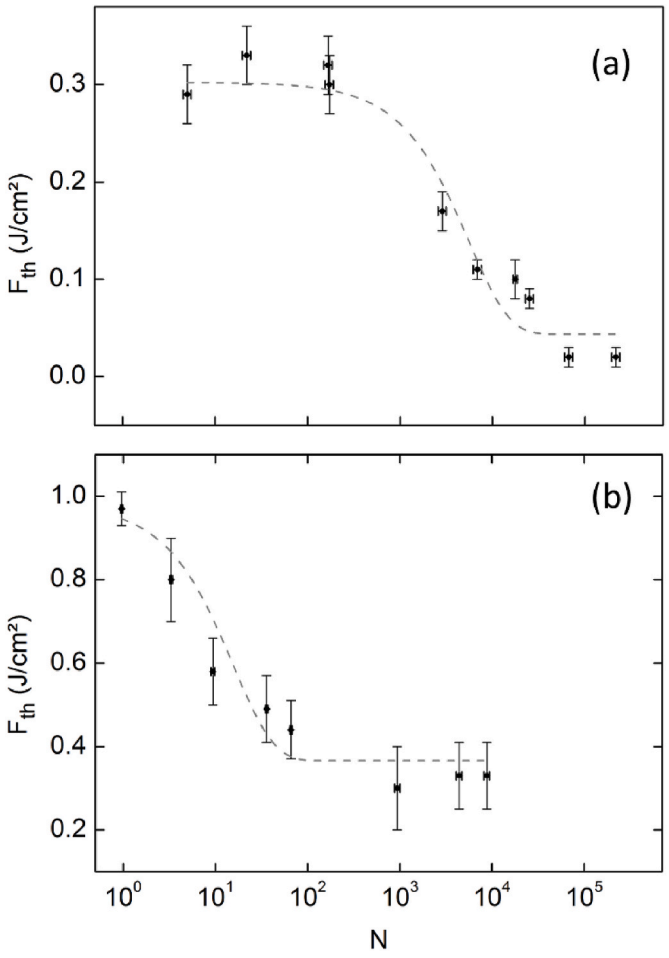

Fig. 3. Incubation effect of L-threonine at 515 nm (a) and 1030 nm (b).

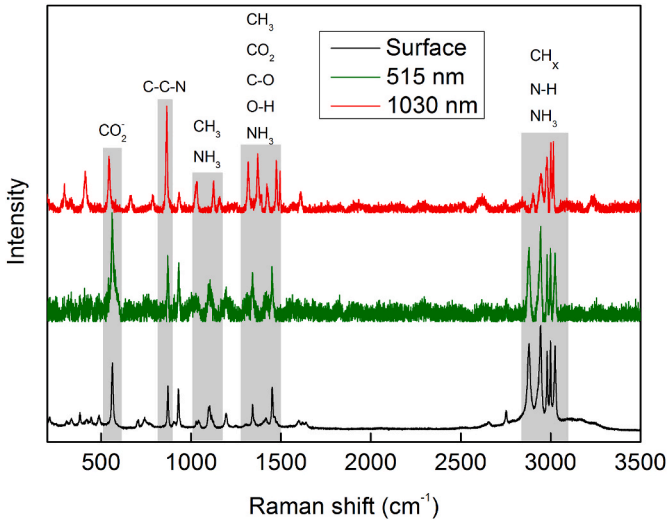

Fig. 4. Micro-Raman spectra at 532 nm of the micromachined structures fabricated at 515 nm (green line), 1030 nm (red line) and in the non-irradiated surface (black line). For clarity, the spectra are shifted along the intensity axis for visualization purposes. (For interpretation of the references to colour in this figure legend, the reader is referred to the Web version of this article.)

fs-laser processing of the material.

4. Conclusions

To summarize, the effect of incubation analysis was explored by femtosecond laser micromachining in L-threonine crystals at 515 nm and 1030 nm, and the damage threshold fluence was determined for one up to 10^5 pulse superposition. In the 1030 nm excitation case, F_{th} decreases from (0.94 ± 0.04) J/cm^2 down to (0.37 ± 0.04) J/cm^2 with ∼ 70 pulses, while at 515 nm, it decreases from (0.31 ± 0.01) J/cm^2 down to (0.05 ± 0.01) J/cm^2 with ∼ 2 × 10^4 pulses, displaying a slower incubation dynamic. Such discrepancy in the damage threshold fluence values at the low pulse superposition region can be explained by the different nonlinear ionization processes: at 515 nm, 3-photon ionization is predominant, while at 1030 nm, 5-photon ionization occurs. In addition, micro-Raman measurements were carried out on the surface of the microstructures produced at the two different wavelengths as well as on the sample's non-irradiated surface, where no noticeable changes were observed on the spectra, indicating that fs-laser micromachining did not induce any substantial structural modifications on the sample. Therefore, the results obtained in this work are an important step towards miniaturized photonic integrated devices in L-threonine crystals via fs-laser micromachining.

Author agreement

We confirm that the manuscript has been read and approved by all named authors and that there is no other person who satisfied the criteria for authorship but is not listed. We further confirm that the order of authors listed in the manuscript has been approved by all of us.

CRediT authorship contribution statement

L.K. Nolasco: Methodology, Investigation, Data Analysis, Writing – original draft, Writing – review & editing. **G.A. Flores:** Methodology, Investigation, Data Analysis, Writing – original draft, Writing – review & editing. **S.N.C. Santos:** Methodology, Investigation, Data Analysis, Writing – original draft, Writing – review & editing. **M.B. Andrade:** Methodology, Investigation, Data Analysis, Writing – original draft, Writing – review & editing. **J.J. Rodrigues:** Resources, Writing – original draft, Writing – review & editing. **C.R. Mendonça:** Methodology, Data Analysis, Writing – original draft, Writing – review & editing, Supervision.

Declaration of competing interest

The authors declare that they have no known competing financial interests or personal relationships that could have appeared to influence the work reported in this paper.

Data availability

Data will be made available on request.

Acknowledgments

We acknowledge Fundação de Amparo à Pesquisa do Estado de São Paulo (FAPESP - 2018/11283-7), Conselho Nacional de Desenvolvimento Científico e Tecnológico (CNPq), Air Force Office of Scientific Research (FA9550-23-1-0664) and Coordenação de Aperfeiçoamento de Pessoal de Nível Superior (CAPES – Finance Code 001) for the financial support. We also thank Professor J.J. Rodrigues Jr. for providing the sample and K.T. Paula for the helpful discussions.

References

[1] D.S. Correa, M.R. Cardoso, V. Tribuzi, L. Misoguti, C.R. Mendonca, Femtosecond laser in polymeric materials: microfabrication of doped structures and micromachining, IEEE J. Sel. Top. Quant. Electron. 18 (2012) 176–186, https://doi.org/10.1109/JSTQE.2011.2106764.

[2] M. Malinauskas, P. Danilevičius, D. Baltriukiene, M. Rutkauskas, A. Žukauskas, Z. Kairyte, G. Bičkauskaite, V. Purlys, D. Paipulas, V. Bukelskiene, R. Gadonas, 3D artificial polymeric scaffolds for stem cell growth fabricated by femtosecond laser, Lith. J. Phys. 50 (2010) 75–82, https://doi.org/10.3952/lithjphys.50121.

[3] N. Takeyasu, T. Tanaka, S. Kawata, Fabrication of 3D metal/polymer microstructures by site-selective metal coating, Appl. Phys. Mater. Sci. Process 90 (2008) 205–209, https://doi.org/10.1007/s00339-007-4298-9.

[4] R.A. Farrer, C.N. LaFratta, L. Li, J. Praino, M.J. Naughton, B.E.A. Saleh, M.C. Teich, J.T. Fourkas, Selective functionalization of 3-D polymer microstructures, J. Am. Chem. Soc. 128 (2006) 1796–1797, https://doi.org/10.1021/ja0583620.

[5] J. Serbin, A. Ovsianikov, B. Chichkov, Fabrication of woodpile structures by two-photon polymerization and investigation of their optical properties, Opt Express 12 (2004) 5221, https://doi.org/10.1364/opex.12.005221.

[6] M. Farsari, A. Ovsianikov, M. Vamvakaki, I. Sakellari, D. Gray, B.N. Chichkov, C. Fotakis, Fabrication of three-dimensional photonic crystal structures containing an active nonlinear optical chromophore, Appl. Phys. Mater. Sci. Process 93 (2008) 11–15, https://doi.org/10.1007/s00339-008-4642-8.

[7] L. Misoguti, A.T. Varela, F.D. Nunes, V.S. Bagnato, F.E.A. Melo, J. Mendes Filho, S. C. Zilio, Optical properties of L-alanine organic crystals, Opt. Mater. 6 (1996) 147–152, https://doi.org/10.1016/0925-3467(96)00032-8.

[8] J.J. Rodrigues, L. Misoguti, F.D. Nunes, C.R. Mendonça, S.C. Zilio, Optical properties of L-threonine crystals, Opt. Mater. 22 (2003) 235–240, https://doi.org/10.1016/S0925-3467(02)00270-7.

[9] S. Boomadevi, K. Pandiyan, Second harmonic generation studies in l-alanine single crystals grown from solution, Phys. B Condens. Matter 432 (2014) 67–70, https://doi.org/10.1016/j.physb.2013.09.048.

[10] F. Pan, M.S. Wong, M. Bösch, C. Bosshard, U. Meier, P. Günter, A highly efficient organic second-order nonlinear optical crystal based on a donor-acceptor substituted 4-nitrophenylhydrazone, Appl. Phys. Lett. 71 (1997) 2064–2066, https://doi.org/10.1063/1.119343.

[11] J.J. Rodrigues, C.H.T.P. Silva, S.C. Zilio, L. Misoguti, C.R. Mendonça, Femtosecond Z-scan measurements of nonlinear refraction in amino acid solutions, Opt. Mater. 20 (2002) 153–157, https://doi.org/10.1016/S0925-3467(02)00062-9.

[12] A.M. Kowalevicz, V. Sharma, E.P. Ippen, J.G. Fujimoto, K. Minoshima, Three-dimensional photonic devices fabricated in glass by use of a femtosecond laser oscillator, Opt. Lett. 30 (2005) 1060, https://doi.org/10.1364/ol.30.001060.

[13] M. Deubel, G. Von Freymann, M. Wegener, S. Pereira, K. Busch, C.M. Soukoulis, Direct laser writing of three-dimensional photonic-crystal templates for telecommunications, Nat. Mater. 3 (2004) 444–447, https://doi.org/10.1038/nmat1155.

[14] R.R. Gattass, E. Mazur, Femtosecond laser micromachining in transparent materials, Nat. Photonics 2 (2008) 219–225, https://doi.org/10.1038/nphoton.2008.47.

[15] S. Kawata, H.B. Sun, T. Tanaka, K. Takada, Finer features for functional microdevices, Nature 412 (2001) 697–698, https://doi.org/10.1038/35089130.

[16] C.N. LaFratta, J.T. Fourkas, T. Baldacchini, R.A. Farrer, Multiphoton fabrication, Angew. Chemie - Int. Ed. 46 (2007) 6238–6258, https://doi.org/10.1002/anie.200603995.

[17] B.N. Chichkov, A. Ostendorf, Two-photon polymerization: a new approach to micromachining, Photon. Spectra. 40 (2006) 72–79.

[18] K.T. Paula, G. Gaál, G.F.B. Almeida, M.B. Andrade, M.H.M. Facure, D.S. Correa, A. Riul, V. Rodrigues, C.R. Mendonça, Femtosecond laser micromachining of polylactic acid/graphene composites for designing interdigitated microelectrodes for sensor applications, Opt Laser. Technol. 101 (2018) 74–79, https://doi.org/10.1016/j.optlastec.2017.11.006.

[19] G.F.B. Almeida, R.J. Martins, J.P. Siqueira, J.M.P. Almeida, J.J. Rodrigues, C. R. Mendonça, Nonlinear optical waveguides inscribed by fs-laser in organic crystal for broadband second harmonic generation of UV pulses, Opt. Mater. 83 (2018) 229–232, https://doi.org/10.1016/j.optmat.2018.06.010.

[20] R. Hanumantha Rao, S. Kalainathan, Impact of ph of L-threonine single crystals on optical parameters and laser damage threshold energy, Int. J. ChemTech Res. 4 (2012) 1478–1484.

[21] R.L. Araújo, M.S. Vasconcelos, C.A. Barboza, J.X. Lima Neto, E.L. Albuquerque, U. L. Fulco, DFT calculations of the structural, electronic, optical and vibrational properties of anhydrous orthorhombic L-threonine crystals, Comput. Theor. Chem. 1170 (2019), https://doi.org/10.1016/j.comptc.2019.112621.

[22] E.A. Davis, N.F. Mott, Conduction in non-crystalline systems V. Conductivity, optical absorption and photoconductivity in amorphous semiconductors, Philos. Mag. A 22 (1970) 903–922, https://doi.org/10.1080/14786437008221061.

[23] J. Tauc, R. Grigorovici, A. Vancu, Optical properties and electronic structure of amorphous germanium, Phys. Status Solidi. 15 (1966) 627–637, https://doi.org/10.1002/pssb.19660150224.

[24] J. Tauc, Optical properties and electronic structure of amorphous Ge and Si, Mater. Res. Bull. 3 (1968) 37–46, https://doi.org/10.1016/0025-5408(68)90023-8.

[25] J.M. Liu, Simple technique for measurements of pulsed Gaussian-beam spot sizes, Opt. Lett. 7 (1982) 196, https://doi.org/10.1364/ol.7.000196.

[26] D.B. Owen, M. Abramowitz, I.A. Stegun, Handbook of mathematical functions with formulas, graphs, and mathematical tables, Technometrics 7 (1965) 78, https://doi.org/10.2307/1266136.

[27] L.K. Nolasco, G.F.B. Almeida, T. Voss, C.R. Mendonça, Femtosecond laser micromachining of GaN using different wavelengths from near-infrared to ultraviolet, J. Alloys Compd. 877 (2021), 160259, https://doi.org/10.1016/j.jallcom.2021.160259.

[28] L.K. Nolasco, F.A. Couto, M.B. Andrade, C.R. Mendonça, Femtosecond laser micromachining study with multiple wavelengths in CVD diamond, Diam. Relat. Mater. 131 (2023), 109589, https://doi.org/10.1016/j.diamond.2022.109589.

[29] G.F.B. Almeida, L.K. Nolasco, G.R. Barbosa, A. Schneider, A. Jaros, I. Manglano Clavero, C. Margenfeld, A. Waag, T. Voss, C.R. Mendonça, Incubation effect during laser micromachining of GaN films with femtosecond pulses, J. Mater. Sci. Mater. Electron. 30 (2019) 16821–16826, https://doi.org/10.1007/s10854-019-01373-2.

[30] L.M. Machado, R.E. Samad, W. de Rossi, N.D.V. Junior, D-Scan measurement of ablation threshold incubation effects for ultrashort laser pulses, Opt Express 20 (2012) 4114, https://doi.org/10.1364/oe.20.004114.

[31] D. Ashkenasi, M. Lorenz, R. Stoian, A. Rosenfeld, Surface damage threshold and structuring of dielectrics using femtosecond laser pulses: the role of incubation, Appl. Surf. Sci. 150 (1999) 101–106, https://doi.org/10.1016/S0169-4332(99)00228-7.

[32] L.V. Keldysh, Ionization in the field of a strong electromagnetic wave, Sov. Phys. JETP 20 (1965) 1945–1957.

[33] C.B. Schaffer, A. Brodeur, E. Mazur, Laser-induced breakdown and damage in bulk transparent materials induced by tightly focused femtosecond laser pulses, Meas. Sci. Technol. 12 (2001) 1784–1794, https://doi.org/10.1088/0957-0233/12/11/305.

[34] G. Ramesh Kumar, S. Gokul Raj, Growth and physiochemical properties of second-order nonlinear optical L-threonine single crystals, Adv. Mater. Sci. Eng. 2009 (2009), https://doi.org/10.1155/2009/704294.

[35] B.L. Silva, P.T.C. Freire, F.E.A. Melo, I. Guedes, M.A. Araújo Silva, J. Mendes Filho, A.J.D. Moreno, Polarized Raman spectra and infrared analysis of vibrational modes in l-threonine crystals, Brazilian J. Phys. 28 (1998) 19–24, https://doi.org/10.1590/S0103-97331998000100003.

[36] A. Pawlukoj, J. Leciejewicz, J. Tomkinson, S.F. Parker, Neutron scattering, infra red, Raman spectroscopy and ab initio study of L-threonine, Spectrochim. Acta Part A Mol. Biomol. Spectrosc. 57 (2001) 2513–2523, https://doi.org/10.1016/S1386-1425(01)00508-X.

[37] K. Machida, A. Kagayama, Y. Saito, Polarized Raman spectra and intermolecular potential of α-glycine-C-d2 and DL-alanine-α,β-d4 crystals, J. Raman Spectrosc. 8 (1979) 133–138, https://doi.org/10.1002/jrs.1250080304.

[38] C.H. Wang, R.D. Storms, Temperature-dependent Raman study and molecular motion in l -alanine single crystal, J. Chem. Phys. 55 (1971) 3291–3299, https://doi.org/10.1063/1.1676579.

[39] H.J. Simpson, R.E. Marsh, The crystal structure of L -alanine, Acta Crystallogr. 20 (1966) 550–555, https://doi.org/10.1107/s0365110x66001221.

[40] K. Machida, A. Kagayama, Y. Saito, Polarized Raman spectra and intermolecular potential of DL-alanine crystal, J. Raman Spectrosc. 7 (1978) 188–193, https://doi.org/10.1002/jrs.1250070405.

[41] M. Ramanadham, S.K. Sikka, R. Chidambaram, Structure of L-asparagine monohydrate by neutron diffraction, Acta Crystallogr. Sect. B Struct. Crystallogr. Cryst. Chem. 28 (1972) 3000–3005, https://doi.org/10.1107/s0567740872007356.

[42] B.L. Silva, P.T.C. Freire, F.E.A. Melo, J. Mendes Filho, M.A. Pimenta, M.S.S. Dantas, High-pressure Raman spectra of L-threonine crystal, J. Raman Spectrosc. 31 (2000) 519–522, https://doi.org/10.1002/1097-4555(200006)31:6<519::AID-JRS567>3.0.CO;2-X.